Journal of Alloys and Compounds 444–445 (2007) 447–452

Journal of ALLOYS AND COMPOUNDS

www.elsevier.com/locate/jallcom

Atomistic level relativistic quantum modelling of plutonium hydrogen reaction

K. Balasubramanian*, Thomas E. Felter, Thomas Anklam, Thomas W. Trelenberg, William McLean II

University of California, Lawrence Livermore National Laboratory, Chemistry and Material Science Directorate, Livermore, CA 94550, United States

Received 28 June 2006; received in revised form 8 November 2006; accepted 9 November 2006
Available online 28 December 2006

Abstract

We have computed the electronic structural and spectroscopic properties for the low-lying electronic states of plutonium hydrides, PuH_n ($n = 2$–4) and their ions which provide significant insight into plutonium hydriding reactions. We have employed a relativistic quantum technique that uses relativistic effective core potentials on Pu. Our computations show that whereas PuH_2 and PuH_3 form stable C_{2v} and C_{3v} structures which exhibit Pu–H direct chemical bonds, PuH_4 becomes a complex of PuH_2 with a partially dissociated H_2. Our computations show that the H_2 dissociation is assisted by PuH_2. Electron density contour maps including Laplacians of charge densities support that the Pu site of the hydrided species is depleted substantially in charge thereby causing catalysis of further hydriding. The IR spectra show that the H_2 sorbed on PuH_2 is partially dissociated. We have also provided comparison of our results with corresponding computations on uranium hydrides.

Keywords: Plutonium hydride; Relativistic quantum modelling; PuH_2; PuH_3; PuH_4

1. Introduction

Actinide hydrogen reactions, particularly those of uranium, plutonium and thorium are quite important in surface and corrosion science of these materials [1] and thus the hydrides of actinides have received considerable attention over many years [1–31]. Some interesting observations pertaining to hydriding is that once hydride is formed further hydrogen reaction seems to take place at a much faster rate. Plutonium seems to exhibit a greater propensity to break the H_2 bond compared to uranium [1]. The product of the hydrogen gas reaction with the materials is pyrophoric actinide hydride layers. The hydrides sites exhibit dramatically greater propensity to cause further hydriding [1,9]. Much of the experimental and theoretical works concerning actinide–hydrogen reactions have been focused on uranium [3–19], especially concerning the thermochemistry, diffusion kinetics and mechanisms of U-hydriding.

Spectroscopic studies of actinide hydrides and oxides have been carried out by Andrews and coworkers [2,21–30] who have studied these species using matrix-isolation techniques by reactions of pulsed laser ablated uranium and thorium atoms with gases such as N_2, O_2, CO_2, H_2 and so on. The primary reaction products of laser-ablated uranium with H_2 gas have been found to be UH_n ($n = 1$–4) and U_2H_n ($n = 2$–4) in a solid argon matrix [24,25]. Likewise Andrews and Cho [2] have recently studied the infrared spectrum and structure of $CH_2{=}ThH_2$ species. Souter et al. [26] have demonstrated that the uranium hydrides are more stable compared to uranium and H_2 gas. In contrast to uranium hydrogen reaction there is less experimental knowledge of the plutonium hydrogen reaction [1].

Theoretical studies actinide containing species have been on the increase [32–44] as the interplay between the 5f and 6d orbitals seems to be quite interesting for actinide species. The phenomenon of "actinide contraction" can be quite important in the chemistry of plutonium and uranium containing species [43,44]. Moreover, relativistic effects are quite significant for actinides and in fact, the actinide contraction is attributed, in part, to relativity as opposed to incomplete shielding of the 5f shells [43,44]. There have been a number of theoretical studies

* Corresponding author. Tel.: +1 925 422 4984; fax: +1 925 422 6810.
E-mail address: balu@llnl.gov (K. Balasubramanian).

0925-8388/$ – see front matter © 2006 Elsevier B.V. All rights reserved.
doi:10.1016/j.jallcom.2006.11.068

on uranium hydrides to understand the relative role of actinide contraction and relativistic effects in the electronic properties of these species. In the present study, we report the results of relativistic computations on the electronic states of PuH_n ($n = 2$–4) and their ions using the density functional theory (DFT) computations employing relativistic effective core potentials on these species.

2. Computational techniques

All computations of PuH_n species were carried out with relativistic effective core potentials (RECPs) that included all but $6s^2 6p^8 4f^6 7s^2$ shells of the Pu atom in the core [43,45]. We have employed the (5s5p4d4f/5s5p3d3f) basis sets for Pu and van Duijneveldt's (5s1p/3s1p) basis set [46] for the hydrogen atoms. We believe that the 5 g functions are unimportant for Pu as the 5f orbitals are core-like in their behavior in plutonium hydrides.

We have employed the density functional (DFT) approach [47–50] that utilized Becke's three-parameter functional [48] with Vosko et al.'s local correlation part [49] and Lee et al.'s [50] nonlocal part (abbreviated as B3LYP). The geometry searches were carried out at the DFT levels using the redundant internal coordinates. We have calibrated the DFT/B3LYP approach earlier for the equilibrium geometries of actinide species, and we have found that the equilibrium geometries are well represented by the DFT/B3LYP/RECP method. The computations were carried out using the GAUSSIAN '03 [51] package of codes.

3. Results and discussion

We have computed the equilibrium geometry and the IR spectra of PuH_n species for the values of $n = 2$–4. Fig. 1 shows the optimized equilibrium geometries of PuH_2 and PuH_2^{2+}. The ground electronic state of PuH_2 was found to be a $^7A_2$ electronic state with a bent equilibrium geometry and a bond angle of 104°. The $^7A_2$ ground state is consistent with two more unpaired electrons in the 5f shell in comparison to the $^5A_2$ ground state of UH_2 [52]. The $^5A_2$ state of UH_2 exhibits U–H bond distances of 2.126 Å and a U–U–H bond angle of 108° at the DFT level [52]. These results compare quite well with the corresponding results for PuH_2 shown in Fig. 1. As can be seen from Fig. 1, the dipositive ion, PuH_2^{2+} exhibits a $^5A_2$ state with considerable elongated Pu–H bond distances of 2.845 Å and thus the Pu–H bonding is weaker in the dication.

The PuH_3 species forms a stable pyramidal equilibrium structure with Pu–H bond distances of 2.081 Å and a pyramidal H–Pu–H bond angle of 112°, as seen from Fig. 1. The ground state of PuH_3 is a $^6A_2$ state as can be seen from Fig. 1. The UH_3 species exhibits an analogous pyramidal structure with U–H bond distances of 2.066 Å and a pyramidal HH–U–H bond angle of 112.3°. However, the ground electronic state of UH_3 [52] is a $^4A_2$ state, as expected since U has two less unpaired electrons in the 5f orbital. Thus, the geometries of the two species are analogous in spite of the electronic states and features being different.

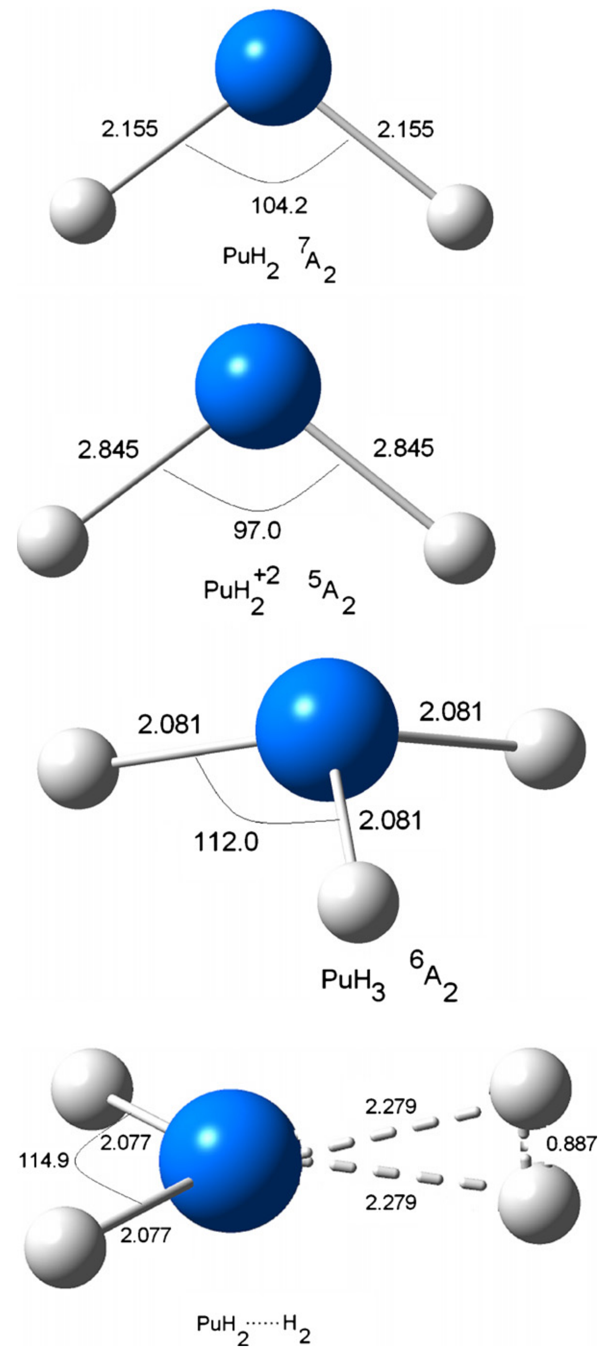

Fig. 1. The optimized equilibrium geometries of PuH_2, PuH_2^{2+}, PuH_3 and PuH_4.

Our results on PuH_4 are quite interesting in that as seen from Fig. 1, PuH_4 forms a distorted structure with two of the hydrogen atoms bonding chemically with Pu. The other two hydrogens are loosely held to Pu but the distances between the hydrogens suggest that the H_2 bond is partially dissociated. It is interesting to note that when started with a tetrahedral PuH_4 species with all four Pu–H bond distances being equal, the optimized structure has a large imaginary vibrational frequency suggesting that the structure would undergo strong distortion. When distortion was allowed, the method of geometry optimization yields the structure shown in Fig. 1. This structure

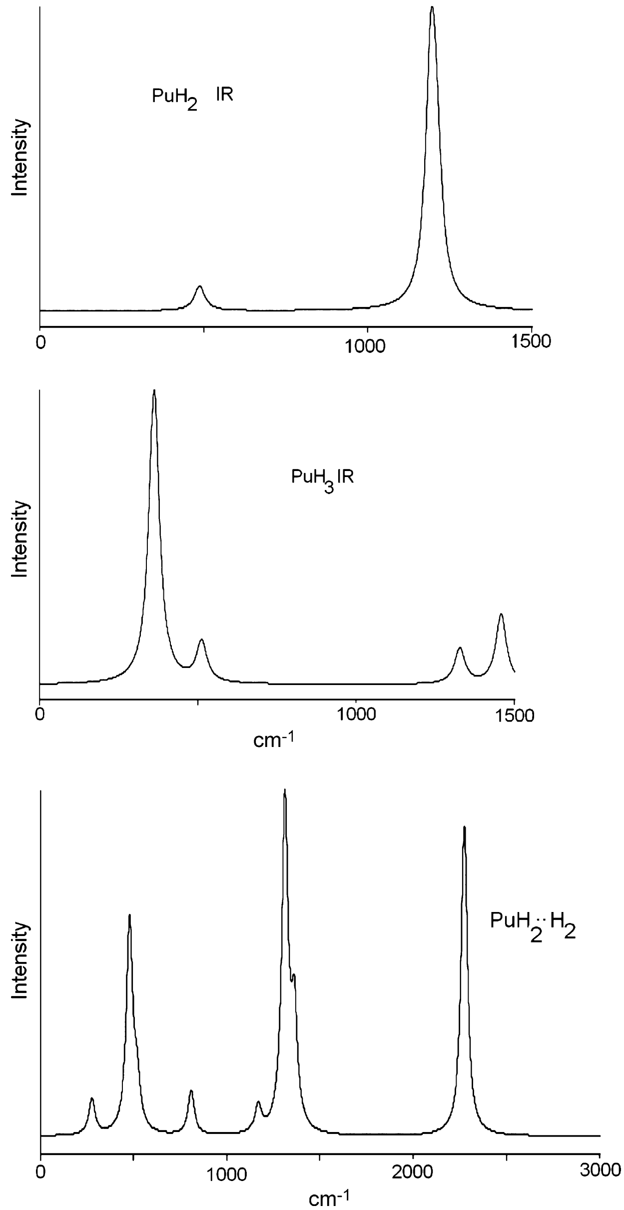

Fig. 2. The computed IR spectra of PuH_2, PuH_3, and PuH_4.

should be viewed as a loose complex of PuH_2 with a partially dissociated H_2. This partial dissociation is achieved by electron density exchanges between highly electron-depleted Pu site when PuH_2 is formed and the additional H_2 molecule. This dative interaction causes partial dissociation of H_2.

Fig. 2 shows our computed IR spectra of PuH_2 and PuH_3 with actual computed vibrational frequencies for all modes in Table 1. The $^7A_2$ state exhibits three vibrational modes, two of which labeled B_2 and A_1 at 1192 and 1208.6 cm^{-1} are quite close and thus show up as a single peak in Fig. 2. The lower frequency A_1 mode corresponds to the bending motion of the hydrogens and appears as a less intense peak at 487 cm^{-1}. The high frequency modes correspond to asymmetric stretch (B_2) and a symmetric stretch (A_1). The PuH_3 IR spectra exhibit more peaks as expected (Fig. 2). The low frequency mode at 363 cm^{-1} is quite intense and corresponds to the motions of hydrogens out of the triangular plane in which they are located at equilibrium. This can be envisaged as concerted inversion motions of the three hydrogens. The peaks at 512 and 1457 cm^{-1} are assigned to E modes while the peak at 1327 cm^{-1} is the A_1 symmetric stretching mode. The peak at 512 cm^{-1} corresponds to a doubly degenerate E representation of the bending motions of hydrogens while the corresponding stretching motions of hydrogens at the higher frequency of 1457 cm$^{-1.}$

The IR spectra of PuH_4 that we have shown in Fig. 2 is quite interesting and striking in that it exhibits an intense peak near 2272 cm^{-1} which is purely a H–H stretching mode of the weakly bound H_2. The frequency is about half of the free H_2 vibrational frequency which is experimentally established as 4401 cm^{-1}. The fact that the frequency is reduced to half the free H_2 frequency is fully consistent with the partially dissociated H_2 sorbed on PuH_2. This is suggestive of catalysis by Pu to dissociate other hydrogens once PuH_2 is formed. There is one more shearing mode of the hydrogens weakly bound to PuH_2 at 2896 cm^{-1}. The other peaks below 1361 cm^{-1} primarily correspond to H–Pu–H modes where the hydrogens are chemically bound to Pu. The weak mode at 1168 cm^{-1} corresponds to a kind of shear vibration of the hydrogens not bonded chemically to PuH_2. The remaining low frequency modes are some kinds of bending or torsional modes involving all four hydrogens. Thus, the IR spectrum of PuH_4 is really that of H_2 physisorbed on to PuH_2.

The dipole moments of PuH_n species reveal an interesting trend. As seen from Table 1, among the species that we have studied here, the PuH_2 species exhibits largest dipole moment consistent with the substantial charge transfer from Pu to the hydrogens. Addition of another hydrogen to PuH_2, which results in the formation of PuH_3, reduces the dipole moment from 5.88 to 4.15 D. That is, three hydrogens compete for the charge transfer from Pu among themselves. The most interesting trend emerges as H_2 is added to PuH_2. The dipole moment dramatically reduces from 5.88 to 1.02 D. This is because the added H_2 molecule competes for charge transfer and since there is considerable charge transfer from Pu to these hydrogens the effective charge transfer to the chemically bonded hydrogens is reduced resulting in a large reduction of the dipole moment.

Table 1
Vibrational frequencies and dipole moments of PuH_n

Species	State	ν_1 (cm^{-1}), intensity	ν_2 (cm^{-1}), intensity	ν_3 (cm^{-1}), intensity	ν_4 (cm^{-1}), intensity	μ_e (D)
PuH_2	$^7A_2$	487: A_1, 78	1192: B_2, 746	1208.6: A_1, 359		5.88
$PuH_2{}^{2+}$	$^5A_2$	233: A_1, 4.7	479.8: A_1, 0.12	484.8: B_2, 0.17		
PuH_3	$^6A_2$	362: A_1, 434.7	512: E, 29.8	1327: A_1, 52.5	1457: E, 57	4.152
PuH_4	$^5A_1$	277: B_2, 1168: B_1, 2272: A1	478: B_1, 1311: B_2, 2896: A_2	518: A_1, 1362: A_1	808: A_1	1.022

The Mulliken populations seem to provide further insight into the nature of these species. The PuH_2 species exhibits Mulliken populations of Pu (0.679), H_1 (−0.339), and H_2 (−0.339). The charges of chemically bonded hydrogens are about −0.34 for PuH_2, and thus about 0.68 charge is depleted from Pu in the case of PuH_2. The PuH_3 Mulliken charges are Pu (1.029), H_1 (−0.343), H_2 (−0.343), and H_3 (−0.343). It is interesting that the Mulliken populations of the three hydrogens in PuH_3 are quite close to the corresponding hydrogen population sin PuH_2. Consequently, Pu is depleted by 1.029 electronic charge due to the presence of three hydrogens. Thus, more charge is depleted on Pu in PuH_3 compared to PuH_2. On this basis then we can predict that an additional H_2 approaching PuH_3 will be partially dissociated due to exchange of charge densities and thus PuH_3 would also assist in further hydriding once it is formed. The PuH_4 species exhibit overall Mulliken charges of Pu (0.955), H_2 (−0.35), H_3 (−0.35), H_4 (−0.128), and H_5 (−0.128), where H_2 and H_3 are chemically bonded hydrogens to Pu. We thus observe that the chemically bonded hydrogens, namely H_1 and H_2 exhibit about the same Mulliken charges as PuH_2. An additional 0.128 electronic charge is donated to physisorbed H_2 to cause partial dissociation. We note that there is dative exchange of charge densities between Pu and hydrogens. The dipositive ions such as PuH_2^{2+} and PuH_3^{2+} have significant positive charges on both Pu and H and thus charge repulsions between Pu and H cause the Pu–H bond lengths to elongate. For example, the Mulliken populations of PuH_2^{2+} are Pu (1.776), H_1 (0.112), and H_2 (0.112), thus both hydrogens are positively charged causing repulsion between Pu and H. Thus, Pu–H bond lengths change from 2.145 to 2.855 for PuH_2 and PuH_2^{2+}, respectively.

The spin densities of the unaired electrons are distributed among the Pu and hydrogen atoms. The heptet state of PuH_2 exhibits distribution of spin densities as Pu (6.163), H_1 (−0.082), and H_2 (−0.082). This suggests strong spin localization on Pu in the case of PuH_2. The quintet state of PuH_3 spin density is distributed among the atoms as Pu (5.34), H_1 (−0.113), H_2 (−0.113), and H_3 (−0.113). There is more delocalization of spin densities in the case of PuH_3. The quartet spin densities of PuH_4 are shared among the atoms as Pu (4.622), H_2 (−0.109), H_3 (−0.109), H_4 (−0.202), and H_4 (−0.202), where H_2 and H_3 are chemically bonded hydrogens to Pu. It is interesting to note that there is greater spin density delocalization on the non-bonded hydrogens which is consistent with partially dissociated nature of H_2 physisorbed on PuH_2.

It is interesting to compare PuH_n with the corresponding UH_n species. Due to two less electrons in U, the electronic states of UH_n exhibit electronic states [52] with two spin multiplicity lower than the corresponding states of PuH_n. The dipole moments of UH_n species are comparable to those of PuH_n. For example, the dipole moment of UH_2 at the DFT level is 6.2 D compared to 5.88 D for PuH_2. The dipole moment of UH_3 is 4.6 D compared to 4.155 D for PuH_3. Thus, the overall dipole moment trends are similar. The Laplacian charge density for PuH_2 is shown in Fig. 3, while UH_3 [52] is shown in Fig. 4 which can be compared to PuH_3 in Fig. 5. We see overall qualitative similarities of the Laplacians of charge densities of other species shown in Fig. 5 in that there are sharp peaks on the actinide metal sites in both cases. With the same scales, PuH_3 shows enhanced activity at the Pu site compared to the U site in UH_3 thereby indicating that Pu would cause dissociation of H_2 to a greater extent once PuH_2 or PuH_3 is formed. Exper-

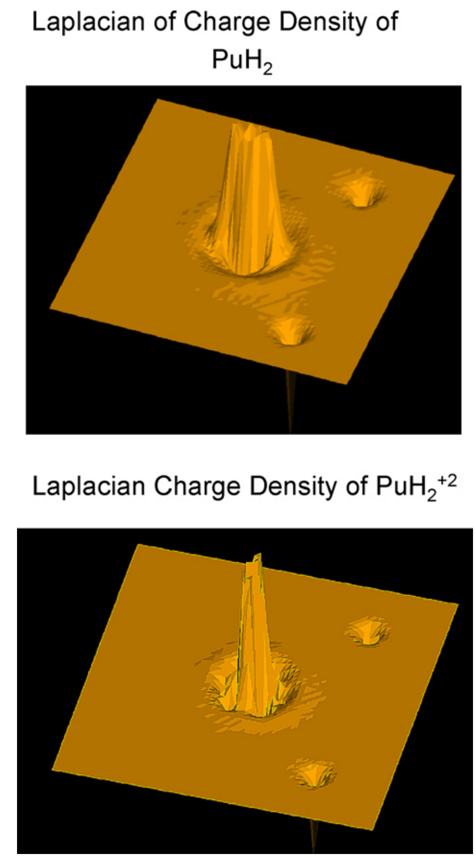

Fig. 3. The Laplacians of charge densities of PuH_2 and PuH_2^{2+}. Peaks at the Pu site indicate electron depleted regions and thus propensity to catalyze further hydriding at the Pu site.

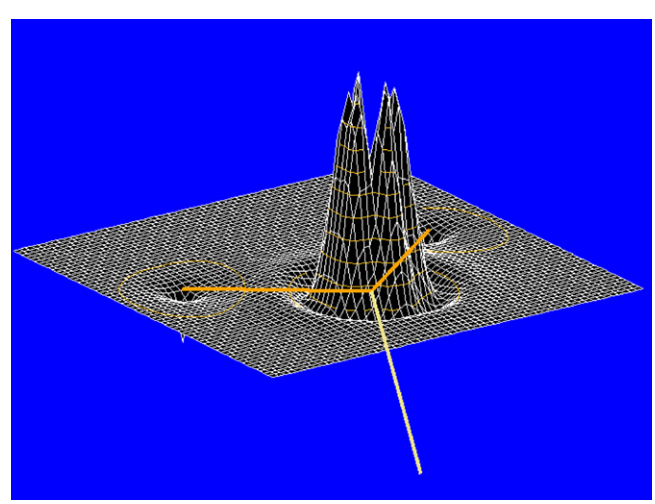

Fig. 4. The Laplacian of the charge density of UH_3, which shows maximal contours at the U site indicating depletion of electronic charge at the U site. In comparison to Fig. 5 for PuH_3, the peaks at the Pu site are denser and concentrated thus Pu is predicted to exhibit greater propensity to cause hydriding.

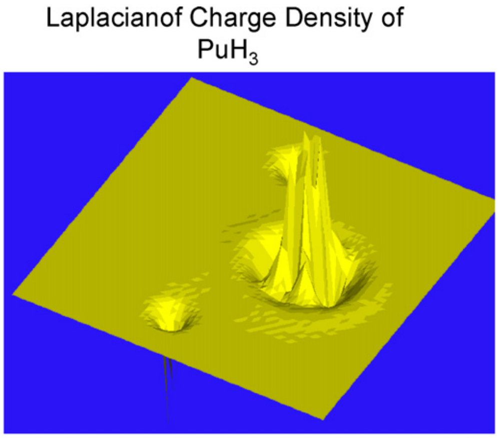

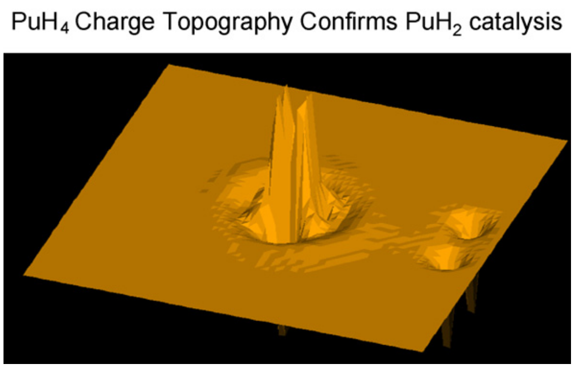

Fig. 5. The Laplacians of charge densities of PuH_3 and PuH_4.

imental studies on Morales and coworkers seem to confirm this trend. The Laplacian of charge density of PuH_4 shown in Fig. 5 is fully consistent with a loose complex of $PuH_2 \cdots H_2$, where we can see two partially dissociated hydrogens exhibiting valleys, are regions of electron density accumulation. The picture is consistent with the partially dissociated H_2.

The spin–orbit effects on PuH_4 can be important since spin–orbit coupling is quite significant for Pu. We have provided estimates to the spin-orbit effects on the basis of the previous study [52] on UH_n species that included spin–orbit effects through a relativistic configuration interaction (RCI) method. The lowest state of UH_2 in the double group is of A_1 symmetry arising predominantly from the $^5A_2$ state. The energy separation of the lowest A_1 state and the second A_1 state including spin–orbit coupling for UH_2 needs to be scaled for PuH_2. Since the spin–orbit effect increases parabolically with Z, we have corrected the spin–orbit splitting of UH_2 with a scaling factor of $(94/92)^2$ in order to obtain the corresponding results for PuH_2. Thus, we obtain the lowest A_1 to second A_1 energy separation of 0.55 eV for PuH_2. The corresponding A_1 to A_2 energy separation is 0.65 eV for PuH_2. We expect the barrier for insertion of Pu into H_2 to be substantially lower for PuH_2 compared to UH_2, and it is also reduced further by spin–orbit coupling so that the dissociation of H_2 on an active Pu site may take place with very little energy barrier or practically no barrier.

4. Conclusion

We have computed the electronic states, equilibrium geometries and IR spectra of PuH_n species for $n = 2$–4. One of the most fascinating results is that PuH_4 does not exist as a tetrahedral species; instead it distorts into a complex of PuH_2 with H_2 where H_2 is partially dissociated and sorbed to PuH_2. Our IR spectra also confirm that H_2 is partially dissociated in this complex. This suggests that once PuH_2 is formed the Pu at the hydrides site becomes an active site for catalysis of further breaking of H_2 molecule in the vicinity. It is thus predicted that the barrier for dissociation of H_2 by PuH_2 would be zero, as H_2 would spontaneously attach to PuH_2 and undergo partial dissociation. This is facilitated by en electron donor–acceptor and back transfer process. The results on PuH_3 and PuH_2 show that these species are chemically bonded with a pyramidal PuH_3 exhibiting a characteristic IR spectra attributable to a pyramidal molecule. Moreover, the inversion motion suggests a rather floppy molecule with a surmountable energy barrier that would make this species non-rigid. The PuH_2 molecule is bent with considerable electronic charge transfer from Pu to hydrogens. The extent of charge transfer per hydrogen is about the same in PuH_2 and PuH_3. On the basis of similarity of bonding between PuH_2 and UH_2 we conclude that the 6d orbitals on Pu are involved in bonding with the H 1s orbitals and that the 5f orbitals so not participate in Pu–H interactions or in the dissociation process of H_2.

Acknowledgement

This work was performed under the auspices of the U.S. Department of Energy by the University of California, Lawrence Livermore National Laboratory under Contract No. W-7405-Eng-48.

References

[1] J.M. Haschke, T.H. Allen, L.A. Morales, Los Alamos Sci. 26 (2000) 252.
[2] L. Andrews, H.-G. Cho, J. Phys. Chem. A 109 (2005) 6796.
[3] D.T. Larson, J.M. Haschke, Inorg. Chem. 20 (1981) 1945.
[4] J.B. Condon, E.A. Larson, J. Chem. Phys. 59 (1973) 855.
[5] J.B. Condon, J. Phys. Chem. 79 (1975) 392.
[6] J.R. Kirkpatrick, J. Phys. Chem. 85 (1981) 3444.
[7] J. Bloch, M.H. Mintz, J. Less Common Met. 81 (1981) 301.
[8] J.R. Kirkpatrick, J.B. Condon, Oakridge National Lab, Internal Report, K/CSD/TM-87, 1990, pp. 1–41.
[9] G.L. Powell, W.L. Harper, J.R. Kirkpatrick, Less Common Met. 172 (1991) 116.
[10] A.L. DeMint, J.H. Leckey, J. Nucl. Mater. 281 (2000) 208.
[11] M.H. Mintz, J. Bloch, Prog. Solid State Chem. 16 (1985) 163.
[12] M. Balooch, A.V. Hamza, J. Nucl. Mater. 230 (1996) 259.
[13] M. Balooch, W.J. Siekhaus, J. Nucl. Mater. 255 (1998) 263.
[14] M.H. Mintz, R. Arkush, A. Venkert, M. Aizenshtein, S. Zalkind, D. Moreno, N. Shamir, M. Brill, J. Alloys Compd. 244 (1996) 197.
[15] D. Moreno, R. Arkush, S. Zalkind, N. Shamir, J. Alloys Compd. 230 (1996) 181;
R. Arkush, M. Brill, S. Zalkind, M.H. Mintz, N. Shamir, J. Alloys Compd. 330 (2002) 472.
[16] T.C. Totemeier, J. Nucl. Mater. 278 (2000) 301.
[17] A. Danon, J.E. Koresh, M.H. Mintz, Langmuir 15 (1999) 5913.

[18] M.R. Castell, S.L. Dudarev, C. Muggelberg, A.P. Sutton, G.A.D. Briggs, D.T. Goddard, J. Vac. Sci. Technol. A 16 (1998) 1055.
[19] C. Muggelberg, M.R. Castell, G.A.D. Briggs, D.T. Goddard, Surf. Sci. 402–404 (1998) 673.
[20] G.C. Allen, I.R. Trickle, P.M. Tucker, Phil. Mag. B 43 (1981) 689.
[21] R.D. Hunt, L. Andrews, J. Chem. Phys. 98 (1993) 3690.
[22] R.D. Hunt, J.T. Yustein, L. Andrews, J. Chem. Phys. 98 (1993) 6070.
[23] T.J. Tague Jr., L. Andrews, R.D. Hunt, J. Phys. Chem. 97 (1993) 10920.
[24] R.D. Hunt, C.A. Thompson, P. Hassanzadeh, L. Andrews, Inorg. Chem. 33 (1994) 388.
[25] P.F. Souter, G.P. Kushto, L. Andrews, Chem. Commun. (1996) 2401.
[26] P.F. Souter, G.P. Kushto, L. Andrews, M. Neurock, J. Am. Chem. Soc. 119 (1997) 1682.
[27] G.P. Kushto, P.F. Souter, L. Andrews, J. Chem. Phys. 108 (1998) 712.
[28] S.P. Wilson, L. Andrews, J. Phys. Chem. 104 (2000) 1640.
[29] M.F. Zhou, L. Andrews, N. Ismail, C. Marsden, J. Phys. Chem. A 104 (2000) 5495.
[30] M.F. Zhou, L. Andrews, J. Li, B.E. Bursten, J. Am. Chem. Soc. 121 (1999) 9712.
[31] P.E. Moreland, D.J. Rokop, C.M. Stevens, Int. J. Mass. Spectrom. Ion Phys. 5 (1970) 127.
[32] P. Pyykkö, Chem. Rev. 88 (1988) 563.
[33] P. Pyykkö, J. Li, N. Runeberg, J. Phys. Chem. 98 (1994) 4809.
[34] P. Pyykkö, J.P. Desclaux, J. Chem. Phys. 34 (1978) 261.
[35] P. Pyykkö, Faraday Trans. II 75 (1979) 1256.
[36] M. Pepper, B.E. Bursten, Chem. Rev. 91 (1991) 719.
[37] M. Pepper, B.E. Bursten, J. Am. Chem. Soc. 112 (1990) 7804.
[38] R.H. Cayton, K.J. Novo-Gradac, B.E. Bursten, Inorg. Chem. 30 (1991) 2265.
[39] K. Balasubramanian, Adv. Met. Semi-Cond. Clusters 2 (1994) 115.
[40] K. Balasubramanian, Handbook on the Physics and Chemistry of Rare Earths, vol. 18, Elsevier Science Publishers, 1994, p. 29.
[41] K. Balasubramanian, J. Chem. Phys. 94 (1991) 1253.
[42] K. Balasubramanian, J. Chem. Phys. 116 (2002) 3568.
[43] K. Balasubramanian, Relativistic Effects in Chemistry. Part A. Theory and Techniques, Wiley/Interscience, New York, NY, 1997, p. 301.
[44] K. Balasubramanian, Relativistic Effects in Chemistry. Part B. Applications to Molecules & Clusters, Wiley/Interscience, New York, NY, 1997, p. 527.
[45] W.C. Ermler, R.B. Ross, P.A. Christiansen, Int. J. Quantum. Chem. 40 (1991) 829.
[46] F.B. van Duijneveldt, IBM Tech. Res. Rep. RF, 1971, p. 945.
[47] R.G. Parr, W. Yang, Density Functional Theory of Atoms and Molecules, Oxford, New York, 1989.
[48] A.D. Becke, J. Chem. Phys. 98 (1993) 5648.
[49] S.H. Vosko, L. Wilk, M. Nusiar, Can. J. Phys. 58 (1980) 1200.
[50] C. Lee, W. Yang, R.G. Parr, Phys. Rev. B 37 (1988) 785.
[51] J. Frisch, G.W. Trucks, H.B. Schlegel, et al., GAUSSIAN '03, Gaussian Inc., Pittsburgh, PA, 1998.
[52] K. Balasubramanian, W. Siekhaus, W. Mclean, J. Chem. Phys. 119 (2003) 5879.